Lasers in Surgery and Medicine 20:22–31 (1997)

Permanent and Transient Changes in the Reflectance of CO_2 Laser-Irradiated Dental Hard Tissues at λ = 9.3, 9.6, 10.3, and 10.6 μm and at Fluences of 1–20 J/cm^2

Daniel Fried, PhD,[1]* Richard E. Glena, BS,[2] John D.B. Featherstone, PhD,[1] and Wolf Seka, PhD[3]

[1]University of California, San Francisco, California 94143-0758
[2]Eastman Dental Center, Rochester, New York 14620
[3]Laboratory for Laser Energetics, University of Rochester, Rochester, New York 14623-1299

Background and Objective: **Effective use of lasers for preventive dental treatments requires accurate knowledge of the amount and distribution of laser energy deposited during irradiation. At CO_2 wavelengths, the reflection losses are considerable and reduce the laser energy absorbed by the tissue surface.**
Study Design/Materials and Methods: **The specular and diffuse reflectance of enamel and dentin were measured at the 10.6-, 10.3-, 9.6-, and 9.3-μm wavelengths of the CO_2 laser. Changes in reflectance during and after laser irradiation were investigated.**
Results: **The low-fluence reflectance (<1 J/cm^2) of calcified dental tissues at CO_2 wavelengths varies between 9% and 50%. Permanent and transient changes in the reflectance are induced at higher irradiation intensities.**
Conclusion: **These changes resulted in increased energy coupling during irradiation. Lasers Surg Med 20:22–31, 1997.**

Key words: carbon dioxide laser; dental tissue; dentin; enamel; tissue optics

INTRODUCTION

Studies have shown that CO_2 lasers can be used effectively to modify the chemical composition and surface morphology of dental enamel and inhibit the progress of subsurface caries-like lesions [1–7]. CO_2 lasers can also be used to ablate carious tissue and have the potential for use for cavity preparations [8,9]. Featherstone and coworkers [3,5,10] studied the effects of low-energy pulsed CO_2 laser radiation on human dental enamel and dentin for laser wavelengths between 9.3 and 10.6 μm. Scanning electron microscopy (SEM) studies [4] showed that the surface effects were highly wavelength dependent in this region and that 9.3 μm and 9.6 μm wavelengths were more efficient at modifying the surface of enamel than the longer CO_2 wavelengths. Those SEM studies [4] suggest that the pulsed CO_2 laser, preferably tuned to the highly absorbed 9.3 and 9.6 μm wavelengths, may be the wavelengths of choice for caries-preventive hard tissue treatments.

Incident light can be either reflected or backscattered from tissue. Reflectance occurs at the surface of tissue and comprises both specular and diffuse components, and the relative quantities are dependent on the surface roughness. Specular reflection is generated for smooth surfaces, while diffuse reflections occur at optically rough interfaces. Backscattered light is not to be confused with diffusely reflected light, which is an interfacial phenomenon; backscattered light

Contract grant sponsor: NIH/NIDR; Contract grant number: DE09958.

*Correspondence to: Daniel Fried, M.Sc., Ph.D., University of California, 707 Parnassus Ave., San Francisco, CA 94143-0758.

Accepted for publication 25 January 1996.

arises from photons that penetrate the surface of the tissue and are scattered back through the surface. Although dental hard tissue is highly scattering in the visible and near IR, scattering is negligible between $\lambda = 9$ and 11 μm, and all the reflected light is due to Fresnel reflection from the air/tissue interface.

The reflection at the air/sample interface of a dielectric (such as enamel and dentin) is described by the Fresnel reflection formula [11].

$$R = [(n - 1)^2 + k^2]/[(n + 1)^2 + k^2], \quad (1)$$

where n is the refractive index and k is the extinction coefficient. The absorption coefficient (α), k, and the wavelength (λ) are related by the expression $\alpha = 4\pi k/\lambda$. The light reflection and absorption characteristics by solids at or near a strong absorption line or band (molecular vibrational modes in the infrared) can therefore vary markedly.

Dental enamel is primarily carbonated hydroxyapatite, which has strong absorption bands in the infrared region due to phosphate, carbonate, and hydroxyl groups in the crystal structure. There are three vibrational modes (transitions) of the phosphate ion of hydroxyapatite (symmetric and antisymmetric P-O stretching modes) in this region—1,092, 1,040, and 962 cm^{-1} ($\lambda = 9.2$, 9.6, and 10.4 μm, respectively)—which lead to very strong absorption between 9 and 11 μm [12–14]. The spectral output of the CO_2 laser overlaps these strong absorption, bands, and consequently, the reflection and absorption of dentin and enamel vary strongly in this region.

The magnitude of the optical constants n and k of solids at each wavelength can be determined experimentally. However, when k is very large, this measurement is difficult. Duplain et al. [15] estimated the optical constants of bovine enamel at various CO_2 laser wavelengths (9–11 μm) from angularly resolved, polarized reflectance data using the Lorentz model to interpret the data. If the surface of the irradiated tissue is heated sufficiently, the optical constants may change significantly both temporarily and permanently. Furthermore, such changes may increase or decrease the total energy absorbed by the tissue. This may be a result of permanent physical and chemical modification of the enamel or dentin mineral, which occurs in the various phase changes of complex minerals during strong heating [16,17]. Table 1 lists some of the important changes that may significantly alter the reflectance of irradiated and heat-treated enamel and dentin.

TABLE 1. Physical Changes That Occur During the Heating of Tooth Enamel [16,17]

Temperature	Physical and chemical changes
(100–650°C)	Loss of H_2O (~30% of total H_2O content)
	Carbonate loss (~66% of total CO_2 content) and rearrangement of carbonate to phosphate and hydroxyl ion positions
	Pyrolysis of organics
(650–1,100°C)	Sintering and recrystallization
	Formation of β-$Ca_3(PO_4)_2$
	Loss of remaining water and carbonate
(1,280°C)	Melting of hydroxyapatite
(1,450°C)	Hydroxyapatite disproportionates to α′-$Ca_3(PO_4)_2$ and $Ca_4(PO_4)_2O$
(1,600°C)	α′-$Ca_3(PO_4)_2$ and $Ca_4(PO_4)_2O$ melts

In addition to changes in the tissue properties during irradiation, particle ejection and plasma formation during the laser pulse may partially screen the target, thus reducing the amount of energy coupled into the target [18].

For dental hard tissue applications, the reflection and absorption coefficients at the irradiation wavelength are of prime importance. The total energy absorbed, the distance over which the energy is absorbed, and the time interval over which the energy is delivered as well as the thermal properties of the tissue determine the thermal as well as the biological response of the tissue. The high reflectance of these tissues also poses potential hazards during clinical laser treatments which must be addressed. The focus of this report is the measurement of the reflectance of these tissues at the four primary CO_2 laser wavelengths before, during, and after laser irradiation.

MATERIALS AND METHODS

Sample Preparation

For the present study two types of surface finishes were investigated: (a) polished samples and (b) unpolished ("pristine") samples. Polished (planar-parallel) sections of 1–2 mm thickness of bovine enamel and human dentin and enamel (ten each) were prepared from bovine incisors and unerupted extracted human third molars. These sections were polished to a 1-μm finish with embedded diamond discs of 9-, 3-, and 1-μm grit (Rio Grande Inc., Albuquerque, NM). The smear layers on the sample surfaces were removed by sonication. SEM images before and after sonication confirmed that this treatment was effective.

The unpolished samples were hemisectioned tooth crowns of unerupted human third molars that were cleaned with a mild detergent solution to remove any debris from the surface. These unpolished samples were used to determine any differences between polished and unpolished "pristine" enamel samples equivalent to those generally encountered in the clinic.

In addition, samples of synthetic carbonated apatite were prepared by aqueous precipitation according to the method described in Nelson et al. [19,20]. The precipitated apatite was sintered at 900–1,000°C for 2–4 h in a moist CO_2 atmosphere to form a solid nonporous crystalline ceramic disk of carbonated hydroxyapatite [21]. These disks were then polished as described above. Four of the ceramic discs were heated in a furnace for 2 h in air at 600°C and 1,100°C.

For SEM studies, samples were coated with a 12-nm layer of gold and palladium and observed at 50–60,000 × in a JEOL-820 SEM.

Apparatus

The tissue samples were irradiated with a Pulse Systems (Los Alamos, NM) LP-60 CO_2 laser with a pulse duration of 100 μs (see Fig. 2) and wavelengths of λ = 9.3, 9.6, 10.3, and 10.6 μm with a maximum single pulse energy of 250 mJ. At low incident fluences (<1 J/cm^2) the total reflectance, i.e., specular and diffuse component of each sample, was measured as shown in Figure 1a using a 4-in infragold-coated integrating sphere [coating reflectance > 0.97 at 9.3–10.6 μm (Labsphere, North Sutton, NH)]. A similarly coated port was used as a reflectance standard. The signal was recorded by a cooled HgCdZnTe (HCZT) detector (BSA Technology Model PCI-L-2TE-12, Torrance, CA) with integrated preamplifier (~1-μs response time). Signals were then digitized by a Tektronix 2440 digital storage oscilloscope and/or a gated boxcar integrator/averager (Model SRS 250, Stanford Research Systems, Sunnyvale, CA). The laser energy was measured using calorimeters (Model JM584-Scientech, Boulder, CO, and Model ED-200-Gentec, Quebec, Canada).

The specular reflection at both high and low incident fluence was collected at a 30° angle (15° angle of incidence) by the Gentec joulemeter with an active area that subtended a solid angle of 0.032 Sr. The corresponding experimental arrangement is shown in Figure 1b.

The diffusely reflected light at high intensity was measured using a rhodium-coated ellipsoidal reflector with the sample placed at the first focus, f_1 (Fig. 1c). With the sample tilted at an angle of ~40° this arrangement also allowed measurement of both the specular and the diffuse components of the reflected light. This configuration permitted collection of over 70% of the 2π hemisphere above the flat sample (30% is lost through the entrance port of the ellipse). The integrating sphere eliminated alignment problems caused by the small area of the HCZT detector (1 mm^2) as well as the imaging problems associated with the ellipsoidal mirror.

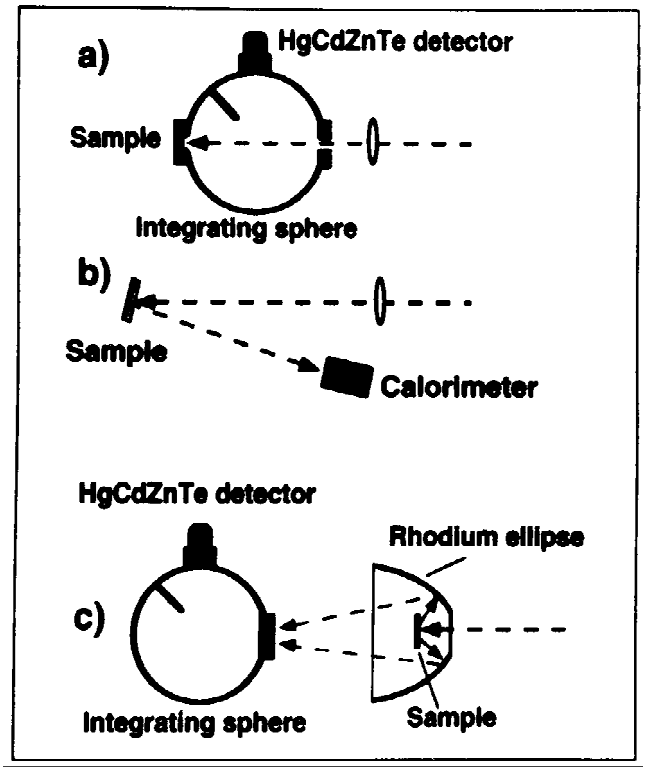

Fig. 1. Experimental setup for measuring the reflected light of irradiated teeth. **a:** Total reflection is measured using a 4-in infragold-coated integrating sphere with a HgCdZnTe detector (HCZT) placed at the port next to the baffle. **b:** Specular reflection measured at an angle of 30° by a Gentec joulemeter (JM). **c:** Diffusely reflected light collected by an integrating sphere and a HCZT detector placed at the secondary focus of the rhodium-coated ellipse.

RESULTS

Polished Dentin and Enamel Samples

The reflectance of human and bovine enamel and human dentin was measured at low incident fluence (<1 J/cm^2) using the integrating sphere (Fig. 1a). The combined specular and diffuse reflectance values of ten polished sections from extracted, unerupted human third molars and ex-

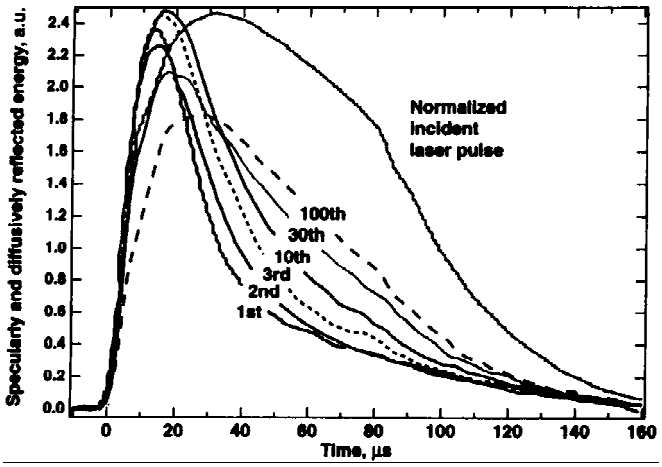

Fig. 2. Time-resolved specular reflection of human dentin as a function of the number of laser pulses at an incident fluence was 18 J/cm^2 at $\lambda = 9.6$ μm, using the setup of Figure 1c. The sample was tilted at 40°, and a 5-mm aperture was placed 60 mm from the sample to collect only the specular reflection. The incident laser pulse was normalized to the peak of the first reflected pulse.

tracted bovine incisors were measured at 9.3, 9.6, 10.3, and 10.6 μm and are listed in Table 2. Our measured values for bovine and human enamel are similar to those published by Duplain et al. [15] for bovine enamel. The reflectance of human dentin is considerably lower than that of human enamel.

For all samples the reflectance at 9.6 μm exceeded the reflectance at the three other wavelengths. This wavelength is close to the P-O stretching vibration (1,040 cm^{-1}, $\lambda = 9.62$ μm) of the phosphate ion in apatite, and the corresponding reflectance exhibited the highest sensitivity to variation of the mineral content. Therefore, we used this wavelength exclusively to study the variability of the reflectance with respect to the sample type. Table 3 lists the reflectance at 9.6 μm and the mineral content of human and bovine enamel, human dentin, and synthetic carbonated hydroxyapatite (CAP) after raising the sample temperature to 600°C and 1,100°C.

Unpolished Samples

The low-intensity (<1 J/cm^2) reflectance of the enamel of unpolished, human third molars was similar in magnitude to the polished samples (five samples unpolished, 48.2 ± 3% at 9.6 μm). There was no variation in the reflection (49 ± 0.7% at 9.6 μm) between wet and dry samples. However, we found that the reflectance could be greatly reduced by surface contaminants (proteins and lipids) on the enamel surface, and we therefore cleaned the surface by brushing with a mild detergent solution.

Polished Carbonated Hydroxyapatite Mineral

Measurements of the low fluence reflectance of CAP after heating in a furnace in air to 600 and 1,100°C were not markedly different from that of unheated CAP, indicating that chemical (e.g., carbonate loss) or physical changes below 1,100°C did not permanently alter the reflectance of the carbonated hydroxyapatite mineral in the 9- to 11-μm wavelength region.

Influence of Internal Scattering

The specularly reflected light (Fresnel reflection) from polished enamel, dentin, and CAP was measured at low incident intensity using the apparatus shown in Figure 1b. The specular reflection did not differ measurably from the total reflectance measured using the integrating sphere setup (Fig. 1a). This eliminates the possibility of significant surface or bulk scattering contributions in stark contrast to the UV, visible, and near IR regions [22,23], where the bulk scattering component is large and absorption is low.

Permanent and Transient Changes in the Reflectance–Multiple Pulse Effects

Typical dental hard tissue treatment with lasers requires multiple pulse irradiation. Therefore, it is of particular interest to characterize any permanent changes in the reflectance that may occur after the first and subsequent laser pulses. At low fluences (<2 J/cm^2 per pulse), the magnitude of the reflectance of dentin and enamel did not change either qualitatively or quantitatively with successive pulses.

For dentin irradiated at fluences above 5 J/cm^2 per pulse at 9.6 μm, there was a permanent increase in the reflectance with successive laser pulses. Reflectance measurements of dentin at fluences greater than 5 J/cm^2 (100-μs pulses, $\lambda = 9.6$ μm) were carried out using the setup of Figure 1c with the sample tilted at 40° to collect the specular as well as the diffuse reflectance (no aperture). Figure 2 shows the evolution of the reflected pulse shapes for multiple pulse irradiation of dentin (18 J/cm^2). The reflectivity increased very rapidly over the first few pulses, after which the reflected pulse stabilized. The duration of the combined specular and diffuse reflectance of the first pulse was considerably shorter than the in-

TABLE 2. Reflectance of Ten Polished Samples of Human and Bovine Enamel and Human Dentin Measured at λ = 9.3, 9.6, 10.3, and 10.6 μm Using the Integrating Sphere (Fig. 1a)

Wavelength	Reflectance of human enamel in percent (standard deviation)	Reflectance of bovine enamel in percent (standard deviation)	Reflectance of human dentin in percent (standard deviation)
10.6 μm	13.2 (0.2)	13.4 (0.5)	8.8 (0.8)
10.3 μm	15.8 (0.1)	15.9 (1.0)	10.3 (0.6)
9.6 μm	49.4 (1.0)	47.2 (1.5)	16.7 (1.5)
9.3 μm	37.7 (0.5)	36.6 (2.2)	8.6 (1.7)

TABLE 3. Comparison of the Reflectance and Mineral Content of Human and Bovine Enamel and Heat-Treated Synthetic Carbonated Hydroxyapatite Mineral (CAP) Measured at 9.6 μm Using the Integrating Sphere Setup of Figure 1a*

Tissue composition	Mineral content by Volume (%)	Reflectance (%)
CAP-25°C	100	47 (s.d. 5%)
CAP-600°C	100	50 (2)
CAP–1,100°C	100	46 (2)
Human enamel	85	49 (1)
Bovine enamel	80	47 (2)
Human dentin	47	17 (2)

*CAP 25°C, 600°C, and 1,100°C represent room temperature CAP (not heated) and CAP that was heated in air to temperatures of 600°C and 1,100°C, respectively.

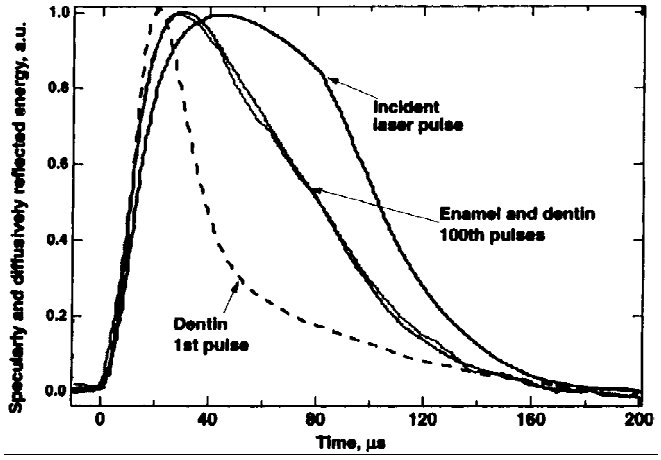

Fig. 3. Temporal evolution of reflected laser light from polished enamel and dentin at λ = 9.6 μm and an incident fluence of 18 J/cm^2. The pulse shapes for the first reflected pulse of dentin (dashed line), the 100th pulse from dentin (dots), and the 100th pulse on enamel (thin solid line) as well as the incident laser pulse shape (thick solid line) were normalized.

cident laser pulse and subsequent reflected pulses. The shape of the reflected pulse gradually broadened and stabilized after 50 to 100 pulses. The time-integrated reflection normalized to the 100th pulse showed an increase in reflectance of 30% over the first 100 pulses. The low fluence reflectance (<1 J/cm^2) of five dentin samples was measured before (18%) and after (23%) irradiation at a fluence of 7 J/cm^2 (λ = 9.6 μm, 50 pulses) and is consistent with the results shown in Figure 2. By contrast, human enamel did not exhibit any permanent changes in the time-integrated total reflectance at these fluences, although the reflected pulse was considerably narrower and differed markedly from the incident laser pulse shape (Fig. 3). After stabilization (100th pulse) the reflected pulse shapes for dentin closely resemble those observed for enamel that do not exhibit any pulse-to-pulse evolution (Fig. 3). The changes in reflectance for dentin may therefore be indicative of the removal of organic material from the vicinity of the surface resulting in a hypermineralized dentin of higher reflectivity.

SEM micrographs of the surface morphology of laser-treated dentin and enamel (100 pulses, λ = 9.6 μm, 18 J/cm^2 incident fluence) at high magnification (60,000×) were virtually indistinguishable (see Fig. 4). The surface morphology exhibited large fused crystals ~500 nm in diameter, much larger than those of normal nonirradiated enamel (40 nm) and dentin (<10 nm). The permanent increase in the reflection of dentin together with the irradiation and SEM observations suggest that the dentin and enamel are converted to similar crystalline hydroxyapatite products through thermal cycling after repeated laser shots. Based on the lack of evolutionary (pulse-to-pulse) changes in the reflectance of enamel, we may conclude that the surface reflection of enamel is almost exclusively governed by the phosphate absorption of the mineral with negligible influence from the organic constituents or surface morphology.

Surface Roughening

While the overall reflectivity of enamel, both time-resolved and time-integrated, exhibited no change from pulse to pulse, the ratio of the

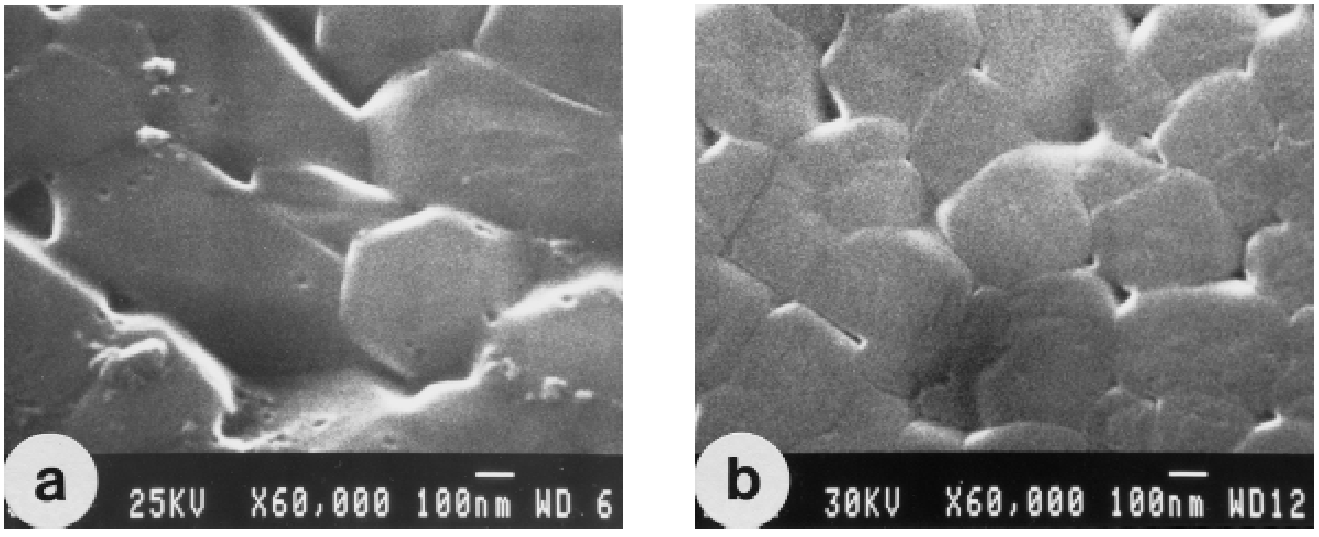

Fig. 4. SEM micrographs (×60,000 magnification) of 9.6-μm CO_2 laser-irradiated enamel and dentin after 20 J/cm^2 incident energy. **a:** One hundred pulses on dentin. **b:** Twenty-five pulses on enamel.

specular to diffuse reflection did exhibit a strong pulse-to-pulse evolution. At fluences greater than 5 J/cm^2 per pulse (100-μs pulses, $\lambda = 9.6$ μm), the specular reflectance of enamel dropped markedly with successive laser pulses, whereas the diffuse reflectance increased commensurably (Fig. 5a,b). Figure 5a shows the time-resolved specular reflectance of human enamel measured by placing the entrance port of the integrating sphere at f_2 of the ellipse (Fig. 1c) and irradiating at 9.6 μm (18 J/cm^2). The sample was tilted at 40°, and the specular reflection was selected with an appropriately placed 5-mm aperture (Fig. 5a). The reflected pulse duration was considerably shorter then the incident laser pulse with the tail end of the pulse significantly attenuated. The time-resolved specular reflectance decreased with a successive number of laser pulses, whereas the time-resolved diffuse reflectance [normal incidence (Fig. 1c)] increased with successive number of laser pulses (Fig. 5b). The diffusely reflected pulse shape also changed dramatically during the initial laser pulses. During the first laser pulse the maximum of the diffuse reflection occurred 40–60 μs after the peak of the incident laser pulse. Apparently the sample surface and optical constants were modified during the first laser pulse, generating the rise in the diffuse reflection from the roughened surface. The delay before the onset of significant diffuse reflection from the first pulse probably relates to the melting of the sample surface with a considerable change in the optical constants and surface quality. A comparison of the reflected pulse shapes of the first two pulses at 9 and 18 J/cm^2 corroborates that the delayed onset in diffuse reflectivity is related to the onset of melting (Fig. 6). The onset of the diffuse reflection occurs much earlier for 18 J/cm^2 than for 9 J/cm^2. SEM images indicate that these energy densities were sufficient to melt and/or vaporize the mineral and that the surface after irradiation exhibited considerable roughness. However, after these chemical and morphological changes, the total overall low-fluence reflectance was not significantly altered from that of unirradiated enamel.

Particle Ejection

During irradiation with 9.6-μm laser light at fluences greater than 5 J/cm^2 for dentin and greater than 9 J/cm^2 for enamel, a strong "white" plume was observed directly in front of the sample. The emission from this plume was measured by imaging it onto the HCZT detector in the direction parallel to the target surface. This signal (Fig. 7) differed markedly from that of the reflected signal, with a peak signal delayed by 40 μs with respect to the incident laser pulse and lasting longer. This delay was consistent with the time lag expected for the ablated particles to leave the surface and appear in the imaged window, suggesting that the origin of the signal is from ejected particulates. The emission from the plume was acquired in the transmission range

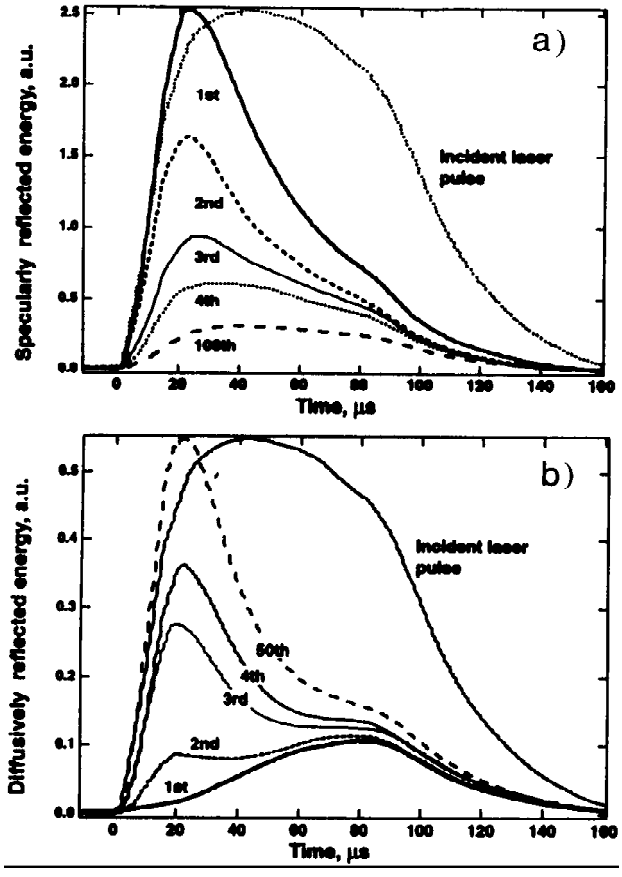

Fig. 5. **a:** Time-resolved specular reflectance of human enamel for multiple pulse irradiation. Incident fluence was 18 J/cm^2 at $\lambda = 9.6$ μm. Measurements were taken using the setup of Figure 1c with the sample tilted at 40° and a 5-mm aperture placed 60 mm from the sample to collect only the specular reflection. **b:** Time-resolved diffuse reflectance of human enamel for multiple-pulse irradiation. Incident fluence was 18 J/cm^2 at $\lambda = 9.6$ μm. Measurement setup used was that of Figure 1c with normal incidence. The incident laser pulses were normalized to the peak of the first and 50th reflected pulses.

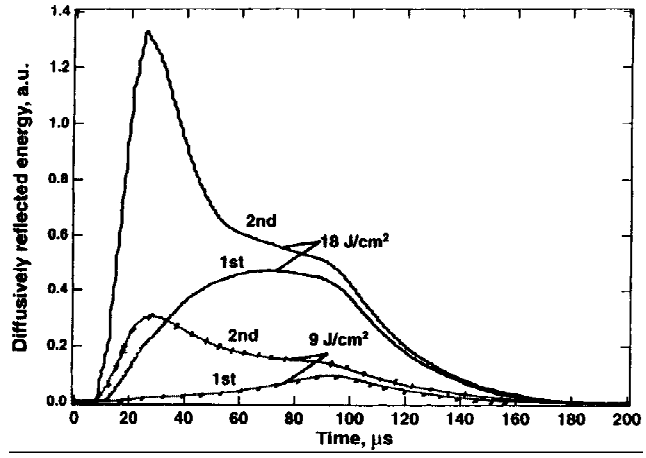

Fig. 6. Time resolved diffuse reflectance of human enamel during the first two laser pulses at an incident fluence of 9 J/cm^2 (dotted lines) and 18 J/cm^2 (solid lines) at $\lambda = 9.6$ μm, measured using setup of Figure 1c with normal incidence.

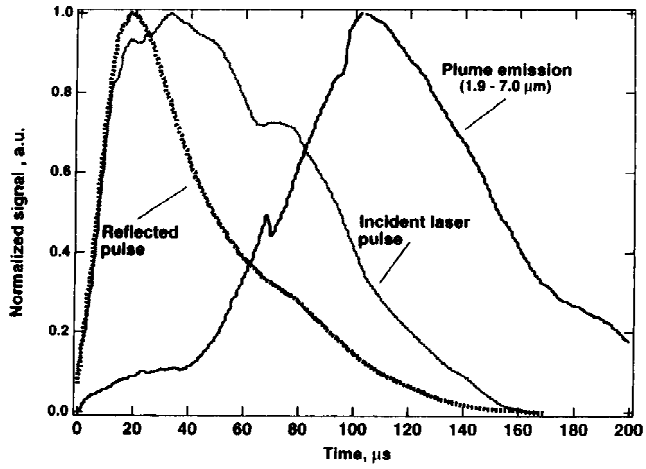

Fig. 7. Normalized temporal evolution of the plume emission, the incident laser pulse, and the reflectance (diffuse and specular) during $\lambda = 9.6$ μm irradiation of human enamel at an incident fluence of 18 J/cm^2. The plume emission was collected parallel to the sample surface using a ZnSe lens and a 1.9- to 7.0-μm bandpass filter, and the reflectance was measured using the setup of Figure 1c.

(1.9–7 μm) and is shown in Figure 7. In contrast, no measurable emission was observed in the transmission range of 5–9 μm. In both cases the spectral filters eliminated the scattered and reflected laser light, removing the possibility that the signal was due to scattered laser radiation. Absence of emission between 5 and 9 μm indicates that this signal was not due to either blackbody radiation from the sample surface or ablated particulates. The 1.9- to 7-μm emission suggests that the source was most likely excited neutral Ca atoms [Ca(I) 1.98 and 1.94 μm [24]] in the ablated plume.

Several experiments employing a second CO_2 laser beam incident parallel to the sample surface (1 mm from the surface) were carried out on both enamel and dentin in an attempt to detect a rise in scattering or absorption due to the plume formed during the ablation of the samples. Such a signal would have confirmed that particulates were shielding the enamel surface. However, under our experimental conditions we were unable to detect any measurable attenuation of the probe beam. By contrast, Forrer et al. [18] investigated the mechanism of CO_2 laser ablation and observed that ejected particles screened the sample

by as much as 60% at fluences greater than 40 J/cm^2 during the CO_2 laser ablation of porcine rib bone. Since dentin is similar in structure and composition to bone, these results appear contradictory. The difference between our results and Forrer's may be partially due to the experimental setup. The geometry of Forrer's setup is likely to emphasize plume shielding, whereas our setup is likely to underestimate it due to plume divergence. Furthermore, our fluences were lower and would therefore be expected to lead to a much smaller plume.

DISCUSSION

Low-Fluence Reflectivity of Enamel, Dentin, and Carbonated Hydroxyapatite (CAP)

The low-fluence reflectance measurements tabulated in Table 2 indicate that the low-intensity reflectance of human and bovine enamel varies strongly over the wavelength range of the CO_2 laser, exceeding 49% at 9.6 μm. These results are consistent with earlier results obtained by Duplain et al. [15] on bovine enamel. Because the reflectance is primarily due to the phosphate absorption, it is directly related to the mineral content of the tissue (Table 3). The reflectance at 9.3 and 9.6 μm of human enamel is slightly higher than for bovine enamel, which is consistent with the slightly higher mineral content of human enamel, i.e., 85% versus 80% by volume for human and bovine enamel, respectively [25].

Low-fluence reflectance measurements of CAP after heat treatment up to 1100°C in a furnace and reflectance studies after high-fluence irradiation (surface temperatures > 1,600°C [26]) reveal little permanent change in the reflectivity. Thus the mineral changes at temperatures less than 1,000°C apparently do not affect the optical properties of the CAP mineral at the common CO_2 wavelengths. This suggests that the secondary calcium phosphate phases, tricalcium and tetracalcium phosphates [16,17,27], formed after the thermal decomposition of tooth enamel, are likely present in only small quantities, and the irradiated (modified) hydroxyapatite has similar reflectance properties.

Dynamic Changes in the Reflectance of Enamel

Above 9 J/cm^2 (9.6 μm) there was obvious particle ejection from enamel (Fig. 7). SEM observations above 10 J/cm^2 produced evidence of some vaporization from the irradiated area (condensed droplets and craters) [28]. The shape of the reflected laser pulse measured during enamel irradiation was considerably narrower than the incident laser pulse and did not change significantly for successive laser pulses. This transient change in the reflectance indicates a change in the absorption properties of the sample during irradiation [28]. This change may be caused by thermally induced changes in the optical constants with increasing temperature and/or a phase transformation, i.e., the liquid phase of hydroxyapatite may have significantly different optical properties then the solid. The optical constants of nonmetallic solids can vary significantly with temperature [29], e.g., the magnitude of the extinction coefficient and the reflectivity at the optical mode frequency of the MgO lattice decreases with temperature between 25°C and 1,000°C; however, the reflectance and extinction coefficients at frequencies lower than the transition frequency can actually increase with temperature because there is a red shift in the optical-mode frequencies with increasing temperature [29]. Assuming that hydroxyapatite behaves in a similar manner, the reflectance of 9.3 and 9.6 μm should decrease with increasing temperature because these wavelengths are on or near resonance, whereas the reflectance at 10.3 and 10.6 μm may increase slightly due to the red shift of the transition frequency.

Dynamic Changes in the Reflectance of Dentin

The changes observed during dentin irradiation were more extensive than those observed for enamel. In addition to the transient changes in the reflectance as a result of laser heating, there were permanent changes in the reflectance, produced by the carbonization and vaporization of the large organic component (30% by mass vs. 4% for enamel).

At fluences greater than 5 J/cm^2 at 9.6 μm the organic component of dentin is preferentially pyrolyzed with successive laser pulses, leaving a mineralized skeleton whose reflectivity increases by 30% during the first 50 laser pulses. This increase is consistent with a rise in the mineral content near the surface as the organic material is pyrolized and removed. SEM studies of the irradiated surfaces at these fluences reveal evidence of considerable surface roughening including cracking, exfoliation, and melting. With the protein and water matrix removed, the modified dentin surface resembles a mineral skeleton of large crystals suggestive of irradiated (modified) enamel.

The shape of the reflected pulse during dentin irradiation changed considerably with number of laser pulses, increasing in width with increasing number of pulses (Fig. 2), and asymptotically approaching the stable pulse shape measured for enamel (Fig. 3). Expansion and pyrolysis of the organic and water content of dentin are expected to occur at temperatures well below the melting temperature of the mineral component (1,200°C). The rapid expansion of these materials below the surface of the tooth may explosively remove overlying mineral [18]. Ejected particles may interfere significantly with the incident laser pulse, generating the reflected pulse shape dependency observed after dentin irradiation (Fig. 3). The ablated particles are thermally isolated from the sample, and they can therefore be heated to very high temperatures and can be fragmented and atomized by the incoming laser pulse, generating the visible white glow and the 1.9- to 7-μm emission of Figure 7.

CONCLUSIONS

Our present and previous studies [15] indicate that the low-fluence reflectance (<1 J/cm^2) of calcified dental tissues at carbon dioxide wavelengths varies between 9% to 50%. The high reflectance must be taken into account in any laser treatment requiring accurate knowledge of the irradiation dose, which applies to preventive treatments. Due to the high reflectivity, particularly at the 9.3- and 9.6-μm wavelengths, stray reflections can be significant and may be a safety concern.

At higher fluences, permanent and transient changes in the reflectance are induced as a result of changes in the optical constants with temperature and the carbonization and vaporization of the organic constituents. These variations are significant and can result in increased or decreased coupling of the incident laser energy to the tissue. Both the transient and permanent changes in reflectance during and after irradiation must be considered in evaluating the energy deposition in these tissues, particularly for the strongly absorbed wavelengths of 9.3 and 9.6 μm.

ACKNOWLEDGMENTS

This work was supported by NIH/NIDR grant DE09958. The contributions of Sandra M. McCormack in the conduct of the SEM work and Scott F. Borzillary are acknowledged with thanks.

REFERENCES

1. Stern RH, Sognnaes RF, Goodman F. Laser effect on *in vitro* enamel permeability and solubility. J Am Dent Assoc 1966; 78:838–843.
2. Melcer J. Latest treatment in dentistry by means of the CO_2 laser beam. Lasers Surg Med 1986; 6:396–398.
3. Nelson DGA, Jongebloed WL, Featherstone JDB. Laser irradiation of human dental enamel and dentine. NZ Dent J 1986; 82:74–77.
4. Nelson DGA, Wefel JS, Jongebloed WL, Featherstone J.D.B. Morphology, histology and crystallography of human dental enamel treated with pulsed low energy IR laser radiation. Caries Res 1987; 21:411–426.
5. Featherstone JDB, Nelson DGA. Laser effects on dental hard tissue. Adv Dent Res 1987; 1:21–26.
6. Fox JL, Yu D, Otsuka M, Higuchi WI, Wong J, Powell GL. Initial dissolution rate studies on dental enamel after CO_2 laser irradiation. J Dent Res 1992; 71:1389–1398.
7. Fox JL, Yu D, Otsuka M, Higuchi WI, Wong J, Powell GL. The combined effects of laser irradiation and chemical inhibitors on the dissolution of dental enamel. Caries Res 1992; 26:333–339.
8. Stern RH, Vahl J, Sognnaes RF. Ultrastructural observations of pulsed carbon dioxide laser effects. J Dent Res 1972; 51:455–460.
9. Walsh JT, Flotte TJ, Anderson RR, Deutsch TF. Pulsed CO_2 laser tissue ablation: effect of tissue type and pulse duration on thermal damage. Lasers Surg Med 1988; 8:108–118.
10. Featherstone JDB, Zhang SH, Shariati M, McCormack SM. Carbon dioxide laser effects on caries-like lesions of dental enamel. Lasers in orthopedic, dental and veterinary medicine. SPIE 1991; 1424:145–149.
11. Cheetham AK, Day P. "Solid State Chemistry Techniques." Oxford: Clarendon Press, 1987.
12. Fowler BO, Moreno EC, Brown WE. Infra-red spectra of hydroxyapatite, octacalcium phosphate and pyrolysed octacalcium phosphate. Arch Oral Biol 1966; 11:477–492.
13. Fowler BO. Infrared studies of apatites. II. Preparation of normal and isotopically substituted calcium, strontium, and barium hydroxyapatites and spectra-structure-composition correlations. Inorg Chem 1973; 13:207.
14. Kravitz LC, Kingsley JD, Elkin EL. Raman and infrared studies of coupled PO_4^{-3} vibrations. J Chem Phys 1968; 49:4600–4610.
15. Duplain G, Boulay R, Belanger PA. Complex index of refraction of dental enamel at CO_2 wavelengths. Appl Optics 1987; 26:4447–4451.
16. Fowler B, Kuroda S. Changes in heated and in laser-irradiated human tooth enamel and their probable effects on solubility. Calcif Tissue Int 1986; 38:197–208.
17. Kuroda S, Fowler BO. Compositional, structural and phase changes in *in vitro* laser-irradiated human tooth enamel. Calcif Tissue Int 1984; 36:361–369.
18. Forrer M, Frenz M, Romano V, Altermatt HJ, Weber HP, Silenok A, Istomyn M, Konov VI. Bone-ablation mechanism using CO_2 lasers of different pulse duration and wavelength. Appl Phys B 1993; 56:104–112.
19. Nelson DGA, Featherstone JDB. Preparation, analysis, and characterization of carbonated apatites. Calcif Tissue Int 1982; 34:S69–S81.
20. Nelson DGA, Barry JC, Shields CP, Glena R, Featherstone JDB. Crystal morphology, composition, and disso-

lution behavior of carbonated apatites prepared at controlled pH and temperature. J Colloid Interface Sci 1989; 130:467–479.
21. Ellies LG, Nelson DGA, Featherstone JDB. Crystallographic structure and surface morphology of sintered carbonated apatites. J Bio Materials Res 1988; 22:541–553.
22. Fried D, Featherstone JDB, Glena RE, Bordyn B, Seka W. The light scattering properties of dentin and enamel at 543, 632, and 1053 nm. In: "Lasers in Orthopedic, Dental, and Veterinary Medicine II," Vol. 1880. Los Angeles, CA: SPIE, 1993, pp 240–245.
23. Fried D, Featherstone JDB, Glena RE, Seka W. The nature of light scattering in dental enamel and dentin at visible and near-IR wavelengths. Appl Optics 1995; 34: 1278–1285.
24. Striganov AR, Sventitskii NS. "Tables of Spectral Lines of Neutral and Ionized Atoms." New York: Plenum, 1968.
25. Curzon MEJ, Featherstone JDB. Chemical composition of enamel. In: Lazzan EP, eds. "Handbook of Experimental Aspects of Oral Biochemistry." Boca Raton, Florida: CRC Press, 1983, pp 123–135.
26. Fried D, Seka W, Glena RE, Featherstone JDB. The thermal response of dental hard tissues to (9–11 μm) CO_2 laser irradiation. Opt Eng; 35(7): 1976–1984.
27. Holcomb DW, Young RA. Thermal decomposition of human tooth enamel. Calcif Tissue Int 1980; 31:189–201.
28. Seka WD, Fried D, Featherstone JDB, Glena RE. Time-dependent reflection and surface temperatures during CO_2 laser irradiation of hard dental tissues with 50–500 μs pulses. In: "Lasers in Dentistry," Vol. 2394. San Jose, CA: SPIE, 1995, pp 51–56.
29. Mitra SS. Optical properties of nonmetallic solids for photon energies below the fundamental band gap. In: Palik ED, eds. "Handbook of Optical Constants of Solids." New York: Academic Press, 1985, pp 213–269.